Journal of
Marine Science
and Engineering

MDPI

Article

Techno-Economic Analysis of NH_3 Fuel Supply and Onboard Re-Liquefaction System for an NH_3-Fueled Ocean-Going Large Container Ship

Jinkwang Lee [1], Younseok Choi [2] and Jungho Choi [1,*]

1 Department of Naval Architecture and Offshore Engineering, Dong-A University, 37 Nakdong-daero 550 Beon-gil, Saha-gu, Busan 49315, Korea
2 Department of Aerospace Engineering, Republic of Korea Air Force Academy, 635 Danjae-ro, Sangdang-gu, Cheongju 28187, Korea
* Correspondence: tamuchoi@dau.ac.kr; Tel.: +82-51-200-7938

Abstract: This study proposed the integrated design of an NH_3 fuel supply system and a re-liquefaction system for an ocean-going NH_3-fueled ship. The target ship was a 14,000 TEU large container ship traveling from Asia to Europe. The NH_3 fuel supply system was developed to feed the liquid fuel at 40 °C and 80 bar and cope with the re-circulated fuel with the sealing oil. Its power consumptions and SECs ranged from 56.4 to 157.5 kW and from 0.0063 to 0.009 kWh/kg, respectively. An onboard re-liquefaction system with a vapor compression refrigeration cycle was also designed to liquefy the BOG from the fuel tank. The re-liquefaction system's exergy efficiency and SEC were 34.71% and 0.224 kWh/kg, respectively. The equipment with the most exergy destruction was the heat exchangers, accounting for 60% of the total exergy destruction. NPV analysis found that it is recommended to introduce the re-liquefaction system to the target ship. At the NH_3 price of USD 250/ton, the reasonable cost of the re-liquefaction system is less than USD 1 million. According to LCC, NH_3 fuel is economically feasible if the carbon tax is more than USD 80/ton and the NH_3 price is around USD 250/ton.

Keywords: NH_3-fueled ship; fuel supply system; re-liquefaction; economic evaluation; NH_3 fuel cost

check for updates

Citation: Lee, J.; Choi, Y.; Choi, J. Techno-Economic Analysis of NH_3 Fuel Supply and Onboard Re-Liquefaction System for an NH_3-Fueled Ocean-Going Large Container Ship. *J. Mar. Sci. Eng.* **2022**, *10*, 1500. https://doi.org/10.3390/jmse10101500

Academic Editor: Viacheslav A. Rudko

Received: 11 September 2022
Accepted: 11 October 2022
Published: 15 October 2022

1. Introduction

The International Maritime Organization (IMO) has imposed stringent environmental regulations on the shipping industry to control the Greenhouse Gas (GHG) emissions from international shipping. Since 1 January 2020, The IMO has set the 2020 sulfur cap, reducing global sulfur emissions to 0.5% from the previous level of 3.5% [1,2]. Consequently, the allowable sulfur content in marine fuels has decreased seven times, from 3.5% to 0.5% of the mass. In order to comply with the IMO low-sulfur policy, many shipping companies should adopt very low-sulfur fuel oil, SOx scrubbers, or LNG [3]. Additional regulations to reduce GHG emissions, such as the Energy Efficiency Design Index (EEDI) and Energy Efficiency Operations Index (EEOI), are being tightened. Along with these de-carbonization efforts, the shipping industry must reduce CO_2 emissions by approximately 90% between 2010 and 2050 to keep the increase in global temperatures below 1.5 °C. In 2018, the IMO Marine Environment Protection Committee (MEPC) set a target to reduce the shipping sector's CO_2 emissions by 50% by 2050, recognizing the shipping sector's enormous contribution to global CO_2 emissions [4].

In 2018, GHG emissions from ships accounted for approximately 2.89% of global emissions. Various methods have been proposed to reduce CO_2 emissions from shipping, including improved hull designs, enhanced power and propulsion systems, increased operational efficiencies, and the use of alternative energies [5]. Furthermore, alternative energy is a viable way to enhance international, national, and regional regulations [6].

H_2 and NH_3 are the most feasible solutions among various alternative energies. The International Transport Forum (ITF) [7] assumes that, in the case of an 80% carbon factor reduction, hydrogen and NH_3 will account for approximately 70% of the fuel market. Moreover, Lewis, J. [8] suggested that H_2 and NH_3 are the most promising zero-carbon fuel options for de-carbonization in the transportation sector. The International Energy Agency (IEA) [9] estimates that H_2 and NH_3 have the potential to meet the environmental target in shipping, but their cost of production is high relative to oil-based fuels.

Table 1 shows the characteristics of H_2 and NH_3 as fuels compared with HFO. Although hydrogen can be obtained from various sources, such as biomass or electrolysis, it is mainly produced from NG [10]. Therefore, its key barriers are the high fuel price and limited availability for maritime operations. In addition, Table 1 shows that H_2 liquefaction requires a relatively low temperature of −253 °C, which gives rise to the high costs of liquefaction and building of storage systems onboard. Furthermore, although H_2 is an environmentally friendly fuel, it is difficult to store due to its low density. The density of LH_2 is approximately 70.8 kg/m^3, and that of heavy fuel oil (HFO) is approximately 1010 kg/m^3. Therefore, NH_3 is currently being discussed as an alternative fuel due to its higher volumetric energy density and ease of handling.

Table 1. Fuel properties of HFO, H_2, and NH_3 [11].

Property	Unit	HFO	Compressed H_2 (350 bar)	LH_2	Liquid NH_3
LHV	MJ/kg	40.2	120	120	18.6
Volumetric energy density	MJ/m^3	39,564–42,036	5040	8500	14,100
Min. auto-ignition temperature	°C	250	500–577	500–577	650–657
Boiling temperature at 1 bar	°C	N/A	N/A	−253	−33.4
Condensation pressure at 25 °C	bar	N/A	N/A	N/A	9.90
Hydrogen content	% mass	N/A	100	100	17.8

NH_3 has a higher volumetric energy density than liquid hydrogen. Although NH_3 has a lower gravimetric energy density (18.6 MJ/kg) compared to H_2 (120 MJ/kg), the density of liquid NH_3 (682 kg/m^3) is significantly higher than that of liquid H_2 (70.8 kg/m^3). Therefore, the volumetric energy density of liquid NH_3 (14,100 MJ/m^3) is higher than liquid H_2 (8500 MJ/m^3), which is one of the advantages to fuel storage onboard. The storage requirements of NH_3 are similar to those of propane; NH_3 is in liquid form at room temperature when pressurized to approximately 10 bar or a temperature of −33.4 °C at 1.013 bar.

Several organizations predict that NH_3 will shortly be considered as a promising alternative fuel for maritime transportation [12]. The American Bureau of Shipping (ABS) identified NH_3 as a zero-carbon fuel that enters the global market relatively quickly and helps meet the GHG emissions profile, regardless of the fuel source [13]. The DNV-GL published a report about NH_3 as a marine fuel, and it is expected that NH_3 will potentially play an essential role in de-carbonizing deep-sea vessels. Although NH_3 is toxic, with an energy density lower than oil-based fuels, it could be a suitable fuel for internal combustion engines [14]. The Korean Register (KR) published a technical report outlining the safety regulations and resulting design implications for NH_3-fueled ships. The report also examines the development status of NH_3 fuel cells and internal combustion engines, analyzing critical international requirements such as the IGC and IGF, which will further influence rule development [15]. In addition, the KR issued the guidelines for a ship using NH_3 as fuel, describing the class society's latest safety regulations and inspection standards for NH_3-fueled vessels [16].

Many studies have been performed on the marine sector's NH_3-fueled internal combustion (IC) engine and fuel supply system. It is worth noting that the main engine and auxiliary engine manufacturers have already started developing new types of engines combusting NH_3 fuel. In 2018, MAN ES announced that the first NH_3 unit could be in operation in a short time based on their LPG engine. Furthermore, MAN ES released the principles of the NH_3-fueled two-stroke engine and the fuel gas supply system [17] and is aiming for the first delivery of a new NH_3-fueled two-stroke engine by 2024 [18]. Furthermore, in 2018, Wartsila signed a memorandum of understanding with Finland's Lappeenranta University of Technology (LUT) and Nebraska Public Power District (NPPD) to develop a generator engine fueled by NH_3 [19]. In 2021, Wartsila and Samsung Heavy Industries (SHI) signed a joint development program agreement to develop NH_3-fueled vessels with four-stroke auxiliary engines [20].

Seo et al. [5] proposed two concepts for NH_3 fuel storage for an NH_3-fueled ammonia carrier and evaluated the concepts in economics. The first concept was to use NH_3 in the cargo tank as fuel, and the second was to install an additional independent fuel tank in the vessel. Kim et al. [11] proposed four propulsion systems for a 2500 TEU container feeder ship, all fueled by NH_3. They consisted of the main engine, diesel generator, proton-exchange membrane fuel cell (PEMFC), and solid oxide fuel cell (SOFC). Compared to the conventional main engine propulsion system with HFO, the SOFC power system was the most eco-friendly. Trivyza et al. [21] suggested the novel NH_3-fueled fuel cell system, and a safety analysis and the preliminary HAZID were performed. In addition, the proposed system's critical faults and functional failures were identified, and the system's reaction to the identified hazards was assessed. Kjeld Aado [22] introduced the principles of the NH_3-fueled MAN ES two-stroke dual-fuel engines. The NH_3 fuel supply system was proposed, similar to the LPG supply system, and the NH_3 fuel specifications were described for the two-stroke engine. Duong et al. [23] designed a novel integrated system with SOFCs and a gas turbine (GT) and evaluated it thermodynamically.

A survey of the existing literature and research shows that, despite optimistic demand forecasts and industrial interest in NH_3-powered ships, there is a lack of comprehensive studies and analyses on the NH_3 fuel supply system for NH_3-powered applications. Therefore, the present study proposes a novel design of the NH_3 fuel supply system with an onboard NH_3 re-liquefaction system in an ocean-going 14,000 TEU container vessel, considering the technical and economic aspects of a deep-sea vessel. This study takes the following approach: First, the target vessel and its appropriate fuel tank are reasonably selected for oceanic conditions, and its potential operation profile is considered. Second, an integrated design of the NH_3 fuel supply system and an NH_3 re-liquefaction system is generated with the selected fuel tank. Third, the onboard re-liquefaction system suitable for NH_3-powered ocean-going vessels is developed and thermodynamically evaluated. Fourth, the economic analysis in this study is performed considering only the annual fuel cost of LNG and NH_3 fuel.

The rest of this paper is organized as follows: First, Section 2 clarifies the design basis and presents an NH_3 fuel supply system and an onboard full re-liquefaction system. Then, the evaluation methodologies—thermodynamic performance and economic feasibility—are explained. Next, in Section 3, the results for the NH_3 fuel supply system and onboard re-liquefaction system are described in detail. Finally, the summary and concluding remarks are presented in Section 4.

2. Materials and Methods

2.1. System Design

This study designs and proposes an NH_3 fuel supply system and an onboard re-liquefaction system using NH_3 as a refrigerant in an NH_3-powered large container ship equipped with an IMO type-A fuel tank. The NH_3 IC engine utilizes data from the 2-stroke NH_3 engine developed by MAN ES [17]. There is no NH_3-fueled vessel currently in operation, and the LNG storage tank is currently being converted to an NH_3 storage tank or manufactured as an ammonia-ready LNG-fueled vessel. Recently, there are similarities in use, such as approval for the use of NH_3 of existing Mark III LNG systems in GTT [24]; therefore, this study assumed the NH_3 fuel tank based on LNG tanks.

LNG is an alternative and bridge fuel for marine transportation due to its environmental and economic advantages. According to the DNV-GL [25], over 200 LNG-fueled ships have been operating, and 403 more have been on order worldwide since 2000. Currently, as LNG storage tanks for ships are developed to store and transport LNG, there are membrane-type LNG tanks and IMO A-, B-, and C-type independent tanks. Therefore, the membrane type, type-A, and type-B tanks, which can efficiently store a large amount of LNG, are being considered for ocean-going vessels. However, the fuel tanks are not designed to have a high internal pressure, so countermeasures for the generated BOG are required. Additionally, the venting of LNG is not allowed, except in emergencies. Therefore, LNG-fueled ships equipped with membrane, IMO type-A, or type-B fuel tanks handle the boil-off gases (BOGs) as fuel for engines or boilers using BOG compressors [26].

Aspen HYSYS V11 is used as a simulation tool for thermodynamic analysis, with extensive data and robust methods for computing physical properties. In addition, the Peng–Robinson equation of state is applied.

2.1.1. Basis of Design

A Target Ship and Main Engine

This study selected a target ship as a 14,000 TEU container ship sailing to the ocean [19]. Table 2 shows the details of the ship.

Table 2. Details of the target vessel [19].

Specification	Unit	Value
Deadweight, max	DWT	150,000
Scantling draught	m	15.8
Design draught	m	14.5
Length overall	m	368
Length between pp	m	352
Breadth	M	51
Sea margin	%	15
Engine margin	%	15
Light running margin	%	5
Design ship speed	kn	21.5/23.5
Type of propeller	m	FPP
No. of propeller blades	EA	5/6
Propeller diameter	m	9.6–10

The propulsion engine used for this target ship is the 12G90ME-C10.5 engine of MAN ES. Table 3 describes the specifications of the engine. In addition, the nominal continuous revolution (NCR) was assumed to be 85% of the specific maximum continuous revolution (SMCR), and the ship's speed in the NCR was set as 23.5 kts.

Table 3. Specification of the main engine [27].

Main Engine	SMCR, kW	NCR, kW	Speed at NCR, kts	SFOC at NCR, kWh
12G90ME-C10.5	66,353	56,400	23.5	158.9

Specific Fuel Consumptions

The specific fuel consumptions of the engine load from the 12G90ME-C 10.5 engine are listed in Table 4 below. The specific fuel consumption (SFC) of NH_3 and LNG was calculated based on the lower heating value (LHV) of HFO. It is assumed that the LHV of HFO is 42,700 kJ/kg, and the LHV of NH_3 and LNG is 18,600 kJ/kg and 50,000 kJ/kg, respectively.

Table 4. Specific consumption of fuels [27].

Load	Power	SFC, g/kWh		
% SMCR	kW	HFO	LNG	NH_3
100	66,353	165.1	141.0	379.0
95	63,035	162.9	139.1	374.0
90	59,718	160.9	137.4	369.4
85	56,400	158.9	135.7	364.8
80	53,082	158.1	135.0	363.0
75	49,765	157.7	134.7	362.0
70	46,447	155.2	132.5	356.3
65	43,129	153.5	131.1	352.4
60	39,812	154.2	131.7	354.0
55	36,494	155.2	132.5	356.3
50	33,177	156.2	133.4	358.6
45	29,859	157.6	134.6	361.8
40	26,541	159.1	135.9	365.2
35	23,224	160.6	137.2	368.7
30	19,906	162.2	138.5	372.4
25	16,588	163.8	139.9	376.0

Operation Profile

The fuel's yearly operational costs greatly depend on the ship's load profile. Container ships typically sail on well-scheduled voyages because it is vital to maintain their schedules. The expected route of the target vessel is from Asia to Europe, and Table 5 proposes an operation profile to estimate the total operating costs per year [19]. The total number of operating days is 280, and since ocean-going container ships tend to run at high speed, more than 65% of the load of SMCR accounts for approximately 80% of the total operating days.

Table 5. Operation profile [19].

Load, % SMCR	Power, kW	Operation Days
100	66,353	14
85	56,400	84
65	43,129	126
50	33,177	14
35	23,224	14
25	16,588	28
Total	-	280

NH_3 Fuel Tank

IMO type-A was selected as the NH_3 fuel tank in this study, and the tank capacity was derived as follows: The design pressure of the NH_3 fuel tank (IMO type-A) is 0.7 barg, which means the NH_3 fuel must be carried in a fully refrigerated condition at or near atmospheric pressure (−33 °C of vapor temperature). With a capacity of 14,861 TEU, CMA CGM Tenere is the first of six Neo-Panamax containers [28]. It is equipped with a 12,000 m^3 LNG fuel tank to complete a roundtrip voyage between Asia and Europe. Assuming the filling limit is 98%, the LNG density is 444.3 kg/m^3, and the LNG LHV is 49,473 kJ/kg, the total energy of the LNG fuel in the tank is 258,492 GJ. Considering the difference in LHV and density between LNG and NH_3 based on the total amount of energy required for the voyage, the mass and volume of NH_3 required were estimated as follows (Table 6). The boil-off rate (BOR) of the 21,064 m^3 NH_3 fuel tank was estimated as 0.04%/day and BOG as 231.6 kg/h [29,30].

Table 6. NH_3 fuel tank sizing [28].

Property	Value	Remark
Required energy, GJ	258,492	12,000 m^3 LNG fuel tank
NH_3 LHV, kJ/kg	18,604	
NH_3 density, kg/m^3	673.1	Liquid saturation at 1.013 bar
Required NH_3 mass, kg	13,894,267	
Required NH_3 volume, m^3	20,643	
NH_3 fuel tank size, m^3	21,064	98% filling limit

2.1.2. Design of NH_3 Fuel Supply System

The NH_3 fuel supply system (FSS) is designed to supply liquid NH_3 fuel at 80 bar and 40 °C to the injection valves of the NH_3 engine [17]. Figure 1 shows the schematic diagram of the fuel supply system. The NH_3 fuel is pressurized up to 25 bar by the submerged pump and heated up to 40 °C through the LP heater. Next, it is pressurized to 80 bar through the high-pressure (HP) pump to supply fuel to the engine. The heating medium of the LP heater is glycol water (water and ethylene glycol). The seawater coolant cools the re-circulated fuel to 38 °C in the return cooler. Finally, the re-circulated fuel with sealing oil is fed back to the fuel through the HP pump.

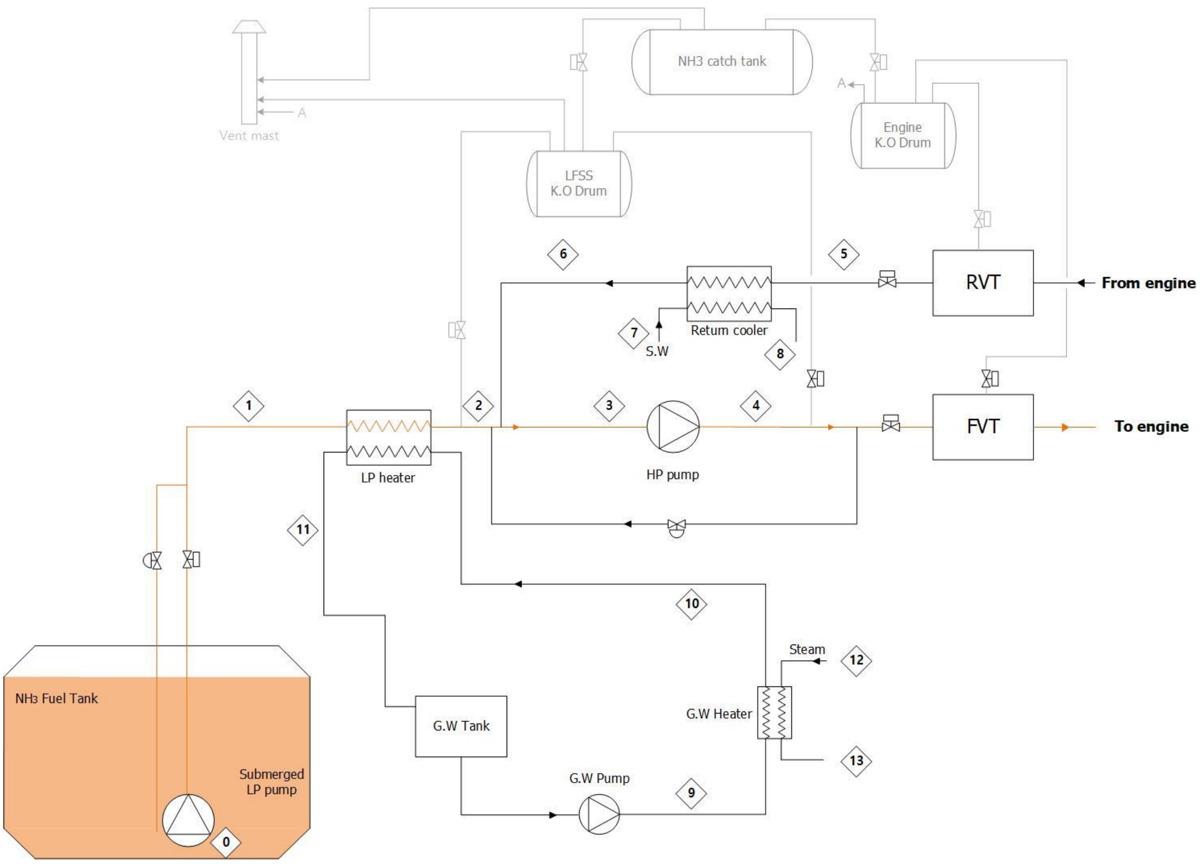

Figure 1. Process flow diagram for NH_3 fuel supply system.

The NH_3 fuel supply system consists of a fuel supply system, a re-circulation system, a fuel valve train system, a nitrogen system, a ventilation system, and an NH_3 capture system [17,22]. This study focuses on the fuel supply system. NH_3 is re-circulated through the re-circulation system to cool down the injection equipment. This re-circulated NH_3 heats up in the engine during operation [17,22]. In addition, the re-circulated fuel contains some of the sealing oil from the injection equipment, which poses a risk of contaminating the fuel tank. The fuel supply system is designed to address the contamination problem by connecting the re-circulation line between the low-pressure (LP) heater and the HP pump.

Moreover, the amount of re-circulated NH_3 varies according to the engine load [31]. When the engine is at a high load, the amount of re-circulated fuel is small compared to the fuel consumption. When the engine is at a low load, the amount of re-circulated fuel is relatively large compared to the fuel consumed. Table 7 shows the re-circulated fuels for fuel consumption. It is assumed that the re-circulated fuel is 20% of the fuel consumption in 100% SMCR, and the re-circulated fuel is 50% of the fuel consumption in 25% SMCR. The remaining re-circulated fuels are derived through the linear regression of these two points.

Table 7. Fuel consumption and re-circulated fuel.

% SMCR	Fuel Consumption, kg/h	Re-circulated Fuel, kg/h
100	25,149.1	1258
95	23,573.2	1413
90	22,058.5	1562
85	20,574.0	1708
80	19,266.1	1837
75	18,016.5	1960
70	16,548.7	2105
65	15,198.2	2237
60	14,093.3	2346
55	13,002.5	2453
50	11,896.9	2562
45	10,803.1	2670
40	9694.0	2779
35	8562.4	2890
30	7412.2	3004
25	6237.7	3119

The following assumptions were made for the simulation of the fuel supply system.

1. The suction temperature and pressure of the submerged fuel pump are −33 °C and 2 bar, respectively.
2. The efficiency of the submerged pump, HP pump, and GW pump is 40%, 75%, and 75%, respectively.
3. The sea water temperature is 32 °C.
4. The temperature and pressure of the re-circulated NH_3 are 50 °C and 80 bar.
5. The pressure drops of the heat exchangers are 0.1 bar.
6. The minimum approach temperature of the return cooler is 3 °C.
7. The GW system is designed to maintain the temperature of its GW outlet at 20 °C.
8. The hydraulic static pressure of the GW expansion tank is neglected.

2.1.3. Design of NH_3 Re-Liquefaction System

BOG caused by heat penetration from the IMO type-A fuel tank during operation is inevitable. The fuel tank pressure should be effectively managed in terms of the fuel tank's structural strength and the fuel quality, which should be maintained at low temperatures. The amounts of BOG generated during voyages are evaporation losses, which are a significant factor in the economics of NH_3-powered fleets. Consequently, the BOG treatment of ships is critical in securing the fleet economy.

Ocean-going vessels have minimal space compared to onshore plants and have low accessibility due to their high sea movement frequency. Therefore, the criteria for an onboard re-liquefaction system are thermodynamic efficiency, compactness, operational simplicity, and easy maintenance. In addition, excessive BOG after the bunkering operation in a terminal is higher than the nominal BOG from the regular voyage. However, it is not considered a design point because the frequency of the bunkering operation is much lower. Table 8 presents the design assumptions for the process simulation of the re-liquefaction system.

Table 8. Design assumptions of BOG re-liquefaction system.

Item	Unit	Value
Boil-off rate	%/day	0.4 [29,30]
BOG	kg/h	231.6 [32]
BOG feed temperature	°C	−20
Suction pressure of BOG compressor	bar	1.4
Composition of BOG	%	NH_3 100

The process flow diagram of the re-liquefaction system is illustrated in Figure 2.

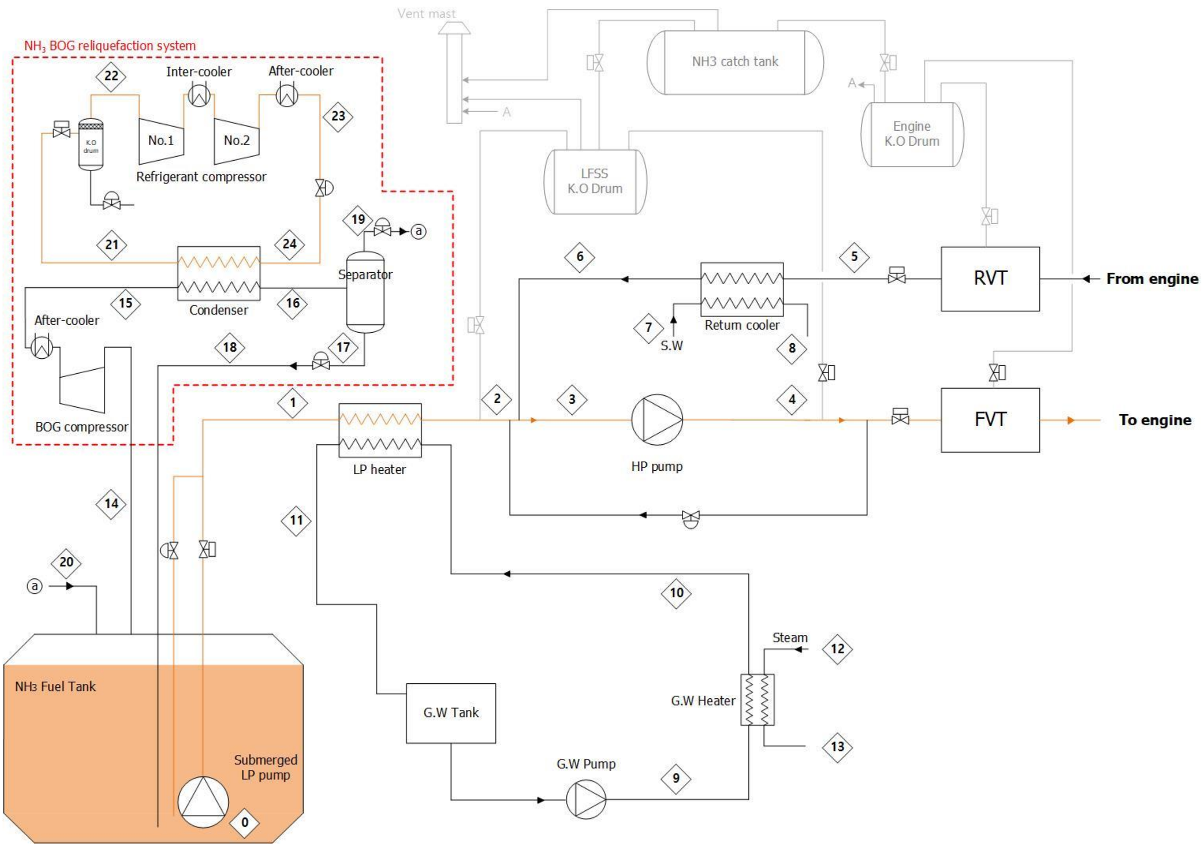

Figure 2. Process flow diagram for NH_3 re-liquefaction system with FSS.

The proposed re-liquefaction system adopts the vapor-compression refrigeration cycle with the NH_3 refrigerant. The BOG is routed into the BOG compressor's suction, so the BOG temperature in the normal voyage is assumed to be −20 °C, which is higher than the fuel storage temperature [32]. The compressed BOG passes through the aftercooler. The BOG with 5 bar and 40 °C passes through the condenser and goes to the tank's bottom with −15.39 °C and 5 bar. In the refrigeration cycle, NH_3 refrigerant is discharged with 15.5 bar and 40 °C by the compressor and the aftercooler. It is delivered to the condenser with −18.53 °C at 2 bar through the J/T valve. The NH_3 refrigerant re-liquefies all NH_3 BOG in this condenser using the latent heat.

For the re-liquefaction cycle analysis, the following assumptions are drawn:

- The minimum temperature approach is 3 °C for the condenser.
- The BOG is composed of 100% NH_3.
- The adiabatic efficiency of the BOG compressors is 75%.

- The pressure ratios for the 1st- and 2nd-stage BOG compressors are 2.5 and 3.1, respectively.
- The aftercooler discharge temperature is 40 °C.
- The pressure drop in the heat exchangers is neglected.

2.2. System Evaluation Methodology

2.2.1. Thermodynamic Performance of NH_3 Fuel Supply System

The NH_3 fuel supply system is an open system that supplies fuel to the engine at the appropriate temperature and pressure with the amount of fuel required by the engine. The rate of NH_3 fuel consumption in the engine varies depending on the ship's speed. Hence, the power consumption of the fuel supply system varies according to the engine load.

The thermodynamic performance of the fuel supply system can be assessed using the required work per unit fuel mass. The specific electric consumption (SEC) is defined using Equation (1).

$$\text{SEC} = \frac{\dot{W}_{total}}{\dot{m}_{fuel}} \tag{1}$$

The total energy for the fuel gas supply is calculated using Equation (2).

$$\dot{W}_{total} = \dot{W}_{Submerged} + \dot{W}_{HP} + \dot{W}_{GW} \tag{2}$$

2.2.2. Thermodynamic Performance of NH_3 Re-Liquefaction System

The thermodynamic performance of the re-liquefaction system can be evaluated using the required work per unit mass of liquefied BOG. SEC is defined by Equation (3) to assess the energy required to re-liquefy 1 kg of BOG.

$$\text{SEC} = \frac{\dot{W}_{net}}{\dot{m}_{RLQ}} \tag{3}$$

The total energy for re-liquefaction is calculated using Equation (4).

$$\dot{W}_{net} = \dot{W}_{BOG} + \dot{W}_{Ref\ 1} + \dot{W}_{Ref\ 2} \tag{4}$$

In thermodynamic physical flow, exergy refers to the maximum useful work delivered to an external user as the stream reaches the dead state. The physical exergy flow is defined by Equation (5).

$$\dot{E} = \dot{m}\cdot e = \dot{m}\cdot[(h_1 + h_0) - T_0\cdot(s_1 - s_0)] \tag{5}$$

where h_1 and s_1 represent the enthalpy and entropy in State 1, respectively, and subscript 0 indicates the standard environmental conditions (1 atm and 25 °C).

Refrigeration systems refer to the reversible and minimum work required for refrigeration to occur at a particular state. During re-liquefaction, the irreversibility between processes causes exergy loss. To estimate the exergy loss, the physical exergy difference between the inlets and outlets of a component can be used. The exergy loss makes the system less efficient and requires more work than the ideal amount. Table 9 presents the equations for calculating the exergy destruction for equipment.

Table 9. Equation of exergy destruction.

Equipment	Exergy Destruction, kW
Compressor	$\dot{E}_{in} + \dot{W}_{input} - \dot{E}_{out}$
Heat exchanger	$\dot{E}_{Cold-in} + \dot{E}_{Hot-in} - \dot{E}_{Cold-out} - \dot{E}_{Hot-out}$
Separator, Valve	$\dot{E}_{in} - \dot{E}_{out}$

From this point of view, the exergy efficiency is a thermodynamic performance evaluation of the re-liquefaction system, defined as the minimum work divided by the actual work in Equation (6).

$$\eta_{ex} = \frac{\dot{E}_{RLQ-out} - \dot{E}_{RLQ-in}}{\dot{W}_{net}} \tag{6}$$

Since no chemical changes are involved in the re-liquefaction system, the total exergy of the system is the physical exergy.

2.2.3. Economic Evaluation

A cost–benefit analysis was performed to assess the economic feasibility of the re-liquefaction system on the NH_3-powered container ship. The results from the study are based on determining whether it is economically feasible. The cost–benefit analysis generally includes methods such as the B/C ratio, Net Present Value (NPV), and Internal Rate of Return (IRR). All three methods provide the same conclusion when there is no change in the discount rate. This study uses NPV to evaluate the economic feasibility of adopting the NH_3 re-liquefaction system as a BOG treatment.

NPV is the difference between the present value of cash inflows and the present value of cash outflows over a period of time. Therefore, it is estimated by subtracting the cost from the benefit with the discount rate (5%) as present values. When the NPV is larger than 0, the profit of a project starts to be generated. Equation (7) shows the mathematical formulation of NPV [18].

$$\text{NPV} = \sum_{t=0}^{L} \frac{B_t}{(1+r)^t} - \sum_{t=0}^{L} \frac{C_t}{(1+r)^t} \tag{7}$$

For the economic feasibility of the integrated system, the NH_3 re-liquefaction system, and fuel supply system, the design of the LNG-powered ship is compared with one of the NH_3-powered ships. For these systems, Life Cycle Cost (LCC) is an appropriate analysis that refers to the ownership cost during the lifetime of a system and is widely used for selecting design alternatives. LCC includes all costs involved in the design, construction, operation, and maintenance. It is calculated in Equation (8) [33].

$$\text{LCC} = \sum_{t=0}^{L} \frac{C_t}{(1+r)^t} = \sum_{t=0}^{0} \frac{\text{CAPEX}_t}{(1+r)^t} + \sum_{t=0}^{L} \frac{\text{OPEX}_t}{(1+r)^t} \tag{8}$$

Capital Expenditure (CAPEX) is defined as the initial investment required to construct a plant, consisting of direct and indirect expenses, contingency, and fees, as shown in Equation (9). The direct expenses include the equipment, material, and labor costs required to install the equipment. The indirect project expenses include the freight, insurance, taxes, and overhead costs needed to construct the plant. The contingency is the cost that covers unforeseen circumstances, whereas the fee is related to the contractors. The direct and indirect expenses are collectively referred to as the bare module cost. The contingency and fee are assumed as 15% and 3% of the bare module cost, respectively. Richard Turton's methodology is used for CAPEX and Operating Expenditure (OPEX) calculations [34].

$$\text{CAPEX} = C_D + C_{ID} + C_{CF} = 1.18 \cdot C_{BM} \tag{9}$$

OPEX is the sum of maintenance, fuel costs, labor, and carbon expenses in Equation (10).

$$\text{OPEX} = C_M + C_F + C_L + C_{CO2} \tag{10}$$

However, although NH_3 fuel for ships is very promising and many research activities are in progress, no actual project has yet been launched. Due to this uncertainty, OPEX considers only the fuel cost, which is usually the most dominant factor in LCC, and CAPEX considers only the purchased equipment cost for fuel supply systems, including fuel tanks. The amount of carbon dioxide emitted when using LNG fuel uses the carbon factor, C_f, which is suggested by the IMO. Equation (11) shows the carbon factor of LNG [35]. Sensitivity analyses for NH_3 prices and carbon dioxide taxes are also performed.

$$C_f = 2.75(ton{\cdot}CO_2/ton{\cdot}LNG) \tag{11}$$

The carbon emission costs are added to the NPV and LCC analysis to demonstrate how they would affect the economic viability. They may be estimated as shown in Equation (12).

$$C_{CO2} = M_{CO2}{\cdot}R_{TAX} \tag{12}$$

For the economic analysis, the following assumptions are drawn:

The power for the operation of the re-liquefaction system is generated by the NH_3 internal combustion generator engine with 50% thermal efficiency.

- The NH_3 fuel consumption for the re-liquefaction system is neglected.
- The LNG price is USD 10 per mmbtu, the price before the Ukraine–Russia conflict in 2022.
- The amount of BOG is constant, 231.6 kg/h, regardless of the ship's operation and the tank's liquid level.
- The lifetime of the target ship is 20 years.
- The re-liquefaction system runs on all operation days, 280 days.
- The discount rate is 5% [36].

3. Results and Discussion

3.1. Thermodynamic Performance of the NH_3 Fuel Supply System

Figure 3 shows the FSS power consumption for the engine loads. The power consumption linearly increases as the engine load increases, ranging from 56.4 kW at 25% of SMRC to 157.5 kW at 100% of SMCR. In addition, the SECs tend to decrease as the engine load increases.

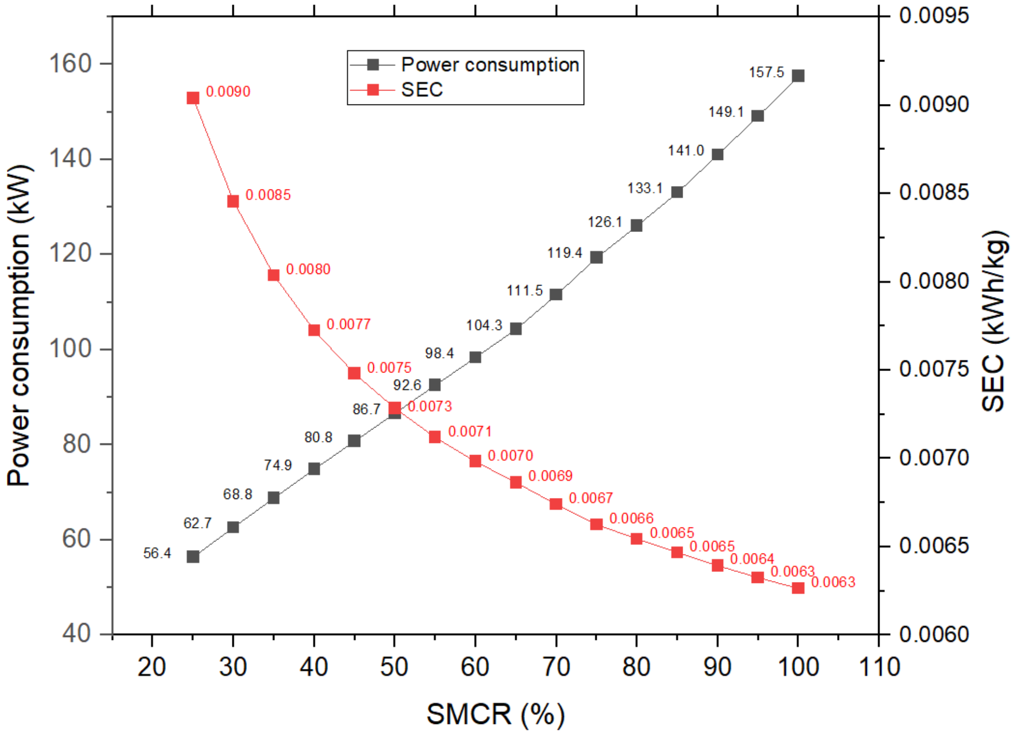

Figure 3. FSS power consumption for % SMCR.

The power consumption of each component is listed in Table 10. The re-circulated NH_3 fuel contaminated with the sealing oil is routed into the suction of the HP pump. This design can address the potential risk of sealing oil freezing in the fuel tank or other tanks, as well as improve the overall power consumption of the NH_3 fuel supply system. The glycol water (GW) system was designed to keep the outlet temperature of the LP heater 20 °C without controlling the system resistance and mass flow. Therefore, the GW pump has a constant power consumption for the engine loads. The inlet GW temperature of the LP heater ranges from 40 °C to 60 °C, which is acceptable.

Table 10. Power consumption for each unit.

% SMCR	Mass Flow, kg/h	GW Pump, kW	HP Pump, kW	Submerged Pump, kW	Total Power, kW	SEC, kWh/kg
100	25,149.1	8.9	99.3	49.3	157.5	0.00626
95	23,573.2	8.9	94.0	46.2	149.1	0.00633
90	22,058.5	8.9	88.9	43.2	141.0	0.00639
85	20,574	8.9	83.8	40.3	133.1	0.00647
80	19,266.1	8.9	79.4	37.8	126.1	0.00654
75	18,016.5	8.9	75.2	35.3	119.4	0.00663
70	16,548.7	8.9	70.2	32.4	111.5	0.00674
65	15,198.2	8.9	65.6	29.8	104.3	0.00686
60	14,093.3	8.9	61.9	27.6	98.4	0.00698
55	13,002.5	8.9	58.2	25.5	92.6	0.00712
50	11,896.9	8.9	54.4	23.3	86.7	0.00728
45	10,803.1	8.9	50.7	21.2	80.8	0.00748
40	9694	8.9	47.0	19.0	74.9	0.00772
35	8562.4	8.9	43.1	16.8	68.8	0.00804
30	7412.2	8.9	39.2	14.5	62.7	0.00846
25	6237.7	8.9	35.3	12.2	56.4	0.00904

3.2. Thermodynamic Performance of NH_3 Re-Liquefaction System

The energy and exergy efficiency were analyzed to evaluate the thermodynamic performance of the re-liquefaction systems. Table 11 shows the SEC and exergy efficiency of the proposed NH_3 re-liquefaction system.

Table 11. Re-liquefaction performances.

Performance Index	Unit	Value
$\dot{W}_{net}$	kW	51.9
$\dot{m}_{RLQ}$	Kg/h	231.6
SEC	kWh/kg	0.224
Exergy efficiency	%	34.71

The amount of nominal BOG is selected as the design point of the re-liquefaction plant. In Figure 2, Stream 14, the suction temperature of the BOG compressor was assumed to be 1.4 bar and −20 °C due to the heat ingress through the pipelines between the top of the fuel tank and the suction of the BOG compressor. The BOG is compressed to 5 bar and fully re-liquefied at −15.4 °C. The re-liquefied NH_3 is transmitted to the bottom of the fuel tank. The re-liquefied 5 bar-NH_3 is expected to be more sub-cooled in the bottom of the fuel tank due to the effect of the hydrostatic pressure of the tank.

In the refrigeration loop, the mass flow rate of the NH_3 refrigerant is 315 kg/h, and it is compressed to 15.5 bar with −40 °C. Next, it flows via the J/T valve. Then, the pressure and temperature are 2 bar and −18.5 °C, respectively. The latent heat of the refrigerant removes the heat, 93.4 kW, of the compressed BOG.

The exergy destruction of each component is essential to exergy analyses and controls the total exergy destruction. Figures 4 and 5 show the exergy destruction and the percentage of the total for each piece of equipment. As expected, heat exchangers are the main components of exergy loss. They account for 60% of the total exergy destruction. The reason for this high exergy loss is the irreversibility of the heat transfer process. The compressors are the second most important factor from the perspective of the exergy loss. They are responsible for 30.1%, and the losses are caused by mechanical irreversibility. The heat exchangers and compressors are the main exergy-destructive components described in Figures 4 and 5. Therefore, it is suggested that more attention should be paid to improving the performance of the heat exchangers and compressors to enhance the exergy efficiency of the re-liquefaction system.

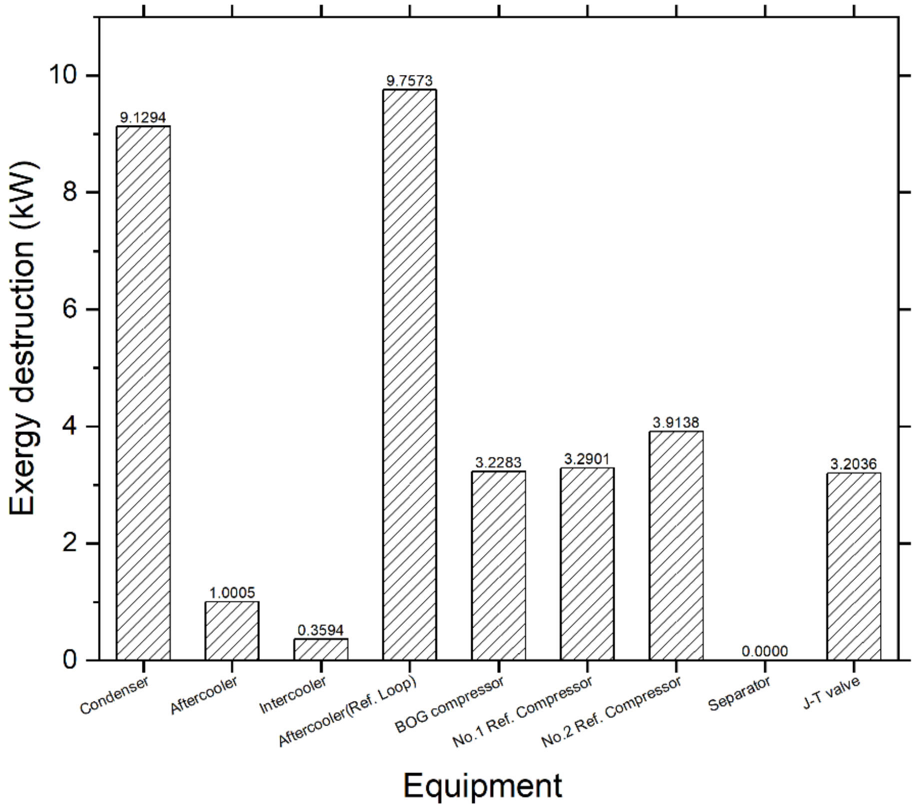

Figure 4. Exergy destruction for each equipment.

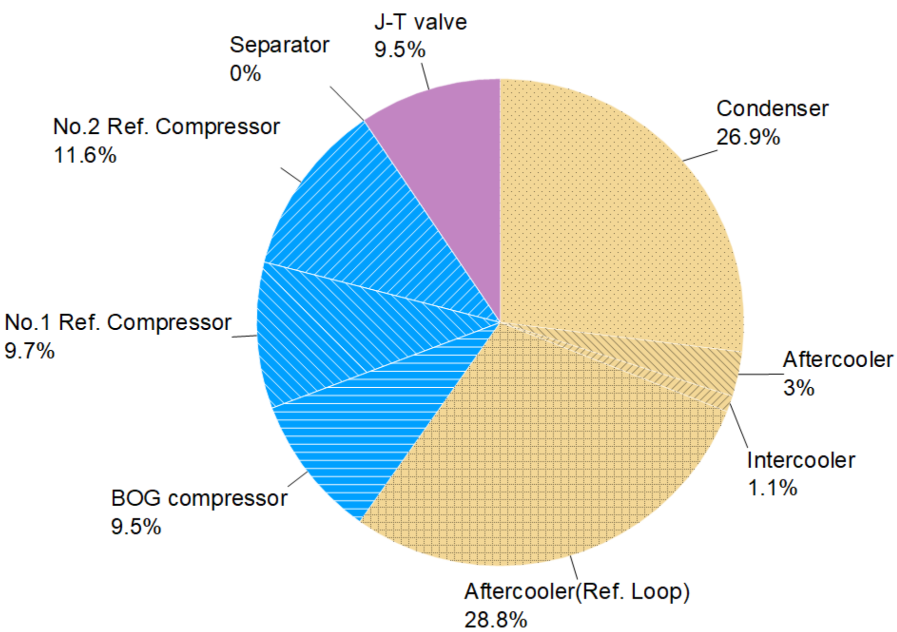

Figure 5. Contribution of each piece of equipment to total exergy destruction.

3.3. Economic Evaluation

3.3.1. NH_3 Re-Liquefaction System

For the economic feasibility of the re-liquefaction system, NPV was performed for the variable NH_3 prices and the variable prices of the re-liquefaction system. The profit was estimated by subtracting the re-liquefaction system's power generation costs from the re-liquefied NH_3 costs. Table 12 shows the operation cost for the re-liquefaction system.

Table 12. Cost for the re-liquefaction system's operation.

NH_3 Price, USD/ton	Power Generation Cost, USD/year
250	33,750
500	67,501
750	101,251
1000	135,001
1250	168,752
1500	202,502

The power consumption for the re-liquefaction system is 51.9 kW.

The amount of annual re-liquefied NH_3 is 1556 tons per year. The cost of the re-liquefied NH_3 varies according to the NH_3 price. Therefore, Table 13 describes the NPV analysis for ten years in the case that the price of the re-liquefaction system is USD 1 million. When the NH_3 is USD 250/ton and USD 500/ton, the profit is generated in the fourth and second years, respectively. If the NH_3 is more than USD 500/ton, the profits are generated from the first year. Consequently, the re-liquefaction system is recommended when the price of the re-liquefaction system is USD 1 million.

Table 13. Annual profit and NPV (the re-liquefaction system: USD 1 million).

Year	NPV					
	NH_3 USD 250/ton	NH_3 USD 500/ton	NH_3 USD 750/ton	NH_3 USD 1000/ton	NH_3 USD 1250/ton	NH_3 USD 1500/ton
1	−661,629	−323,259	15,112	353,482	691,853	1,030,224
2	−339,372	324,172	981,885	1,642,513	2,303,142	2,963,770
3	−32,460	945,936	1,902,621	2,870,162	3,837,702	4,805,243
4	259,838	1,544,624	2,779,513	4,039,351	5,299,188	6,559,026
5	538,216	2,121,800	3,614,648	5,152,864	6,691,080	8,229,296
6	803,338	2,678,186	4,410,015	6,213,353	8,016,691	9,820,029
7	1,055,836	3,213,933	5,167,507	7,223,342	9,279,178	11,335,013
8	1,296,309	3,728,913	5,888,928	8,185,237	10,481,546	12,777,855
9	1,525,332	4,222,957	6,575,995	9,101,327	11,626,659	14,151,991
10	1,743,448	4,696,018	7,230,345	9,973,794	12,717,242	15,460,691
NPV	6,188,856	23,153,279	38,566,569	54,755,425	70,944,282	87,133,138

Figure 6 shows the case when the payback for the prices of the re-liquefaction system and the NH_3 fuel becomes positive. If the payback must start from the third year, it is always satisfied when the price of the re-liquefaction system is USD 0.5 million. If it is USD 1 million and USD 1.5 million and the price of NH_3 is more than USD 500/ton, the payback is generated within the second and third years. If it is USD 2 million, it creates positive profits within the third year when the NH_3 price is more than USD 750/ton. Therefore, it is very reasonable to introduce the re-liquefaction system if it is supplied for less than USD 1 million.

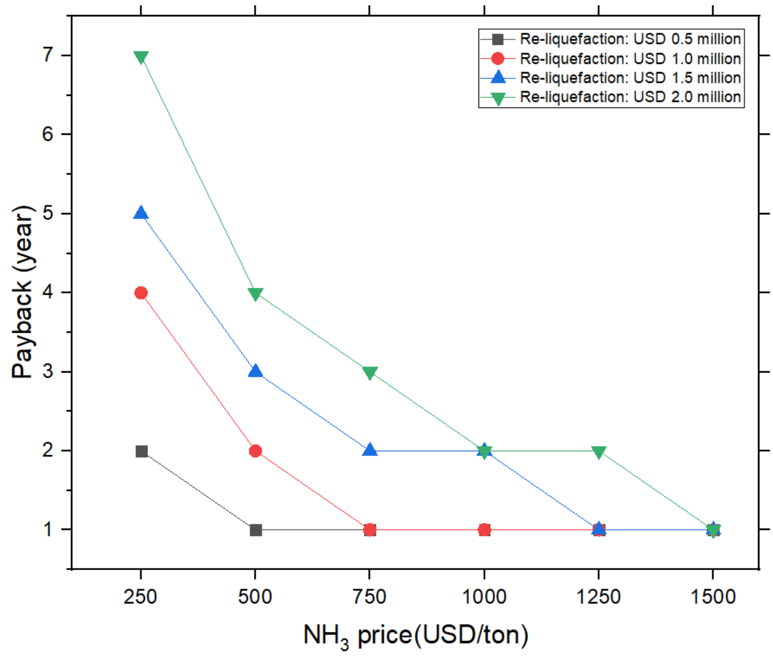

Figure 6. Payback for the NH_3 and re-liquefaction prices.

Figure 7 describes NPVs for the fuel and re-liquefaction system price. The NPV is positive when the re-liquefaction system price is less than USD 1.5 million and negative when the re-liquefaction system price is USD 2 million and the ammonia price is USD 250/ton.

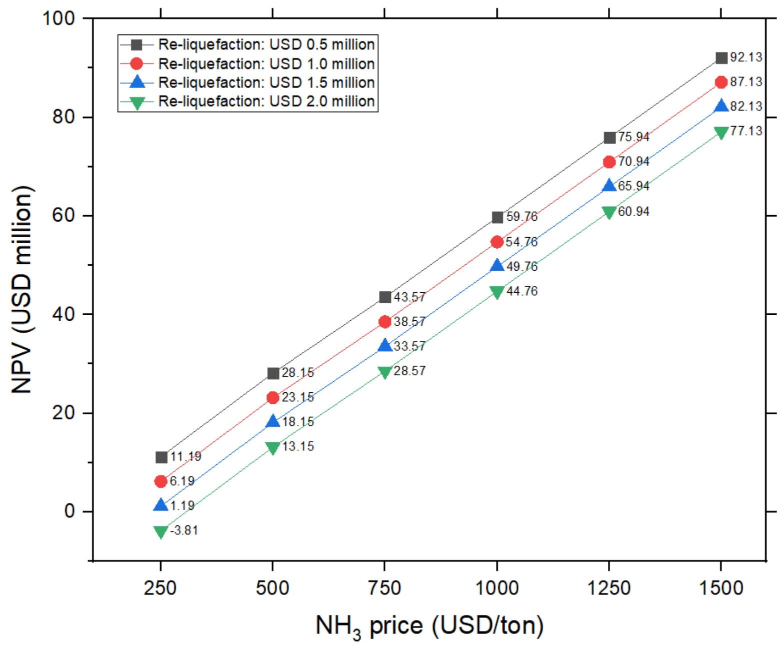

Figure 7. NPV for the NH_3 and re-liquefaction price.

3.3.2. LCC for NH_3 and LNG

The annual fuel consumptions for HFO, LNG, and NH_3 on the engine loads are indicated in Figure 8. The NH_3 fuel has the lowest LHV, so the highest flow rate is required. In Table 14, the total annual fuel consumptions for each fuel are described as the NH_3 fuel consumption of 106,953 tons, the HFO fuel consumption of 46,588 tons, and the LNG fuel consumption of 39,786 tons. These annual fuel consumptions were derived by multiplying the operation days per engine load in Table 5 by the fuel cost per engine load in Figure 8.

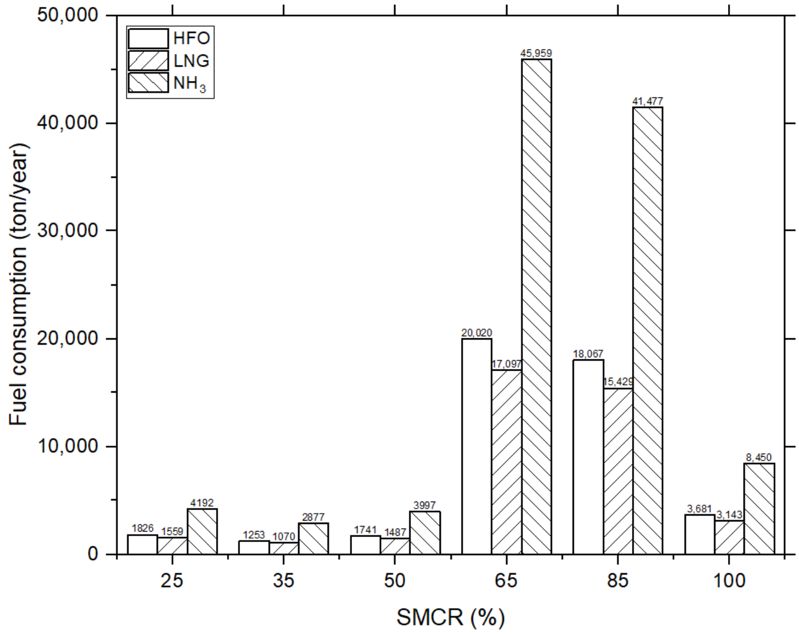

Figure 8. Fuel consumption for the engine loads for HFO, LNG, and NH_3.

Table 14. Annual fuel consumption for fuels.

Annual Operation Days	NH_3 Fuel Consumption, tons	HFO Fuel Consumption, tons	LNG Fuel Consumption, tons
280	106,953	46,588	39,786

NH_3 prices have changed rapidly since the Ukraine–Russia conflict, and to reflect this, sensitivity to changes in NH_3 prices from USD 250/ton to USD 1500/ton was analyzed. Figure 9 shows the annual fuel cost of the target container ship according to the NH_3 prices. If the price of NH_3 is USD 250/ton, USD 26.42 million/year is spent on fuel, and in the case that it reaches USD 1500/ton, USD 16.43 million/year is spent on fuel.

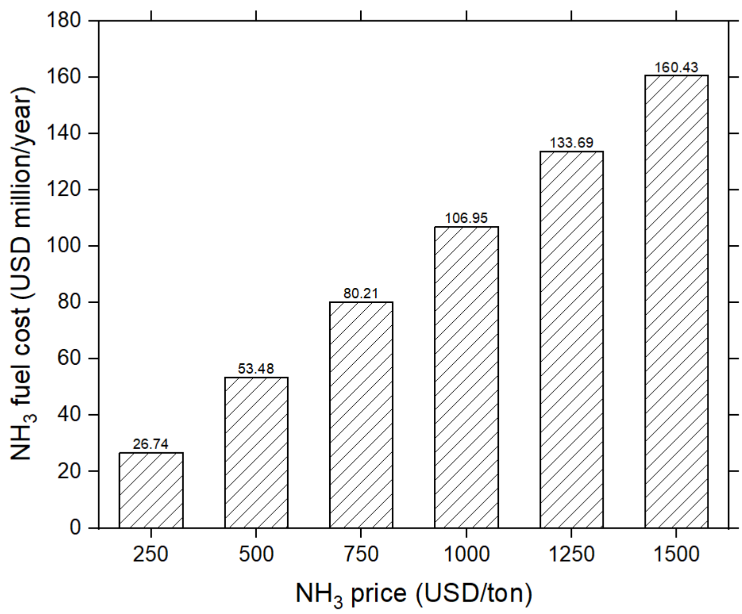

Figure 9. Fuel cost for the NH_3 price.

The target ship's NH_3 and LNG fuel's economic feasibility were investigated, considering CO_2 emissions. Since ammonia fuel does not emit carbon dioxide, CO_2 emissions are considered only for LNG fuel. The annual total CO_2 from the LNG fuel emitted 109,413 tons in the target ship. The LNG price is fixed at the prices before the conflict between Ukraine and Russia. This is because LNG's solid and stable supply chain will likely become stable after the Ukraine–Russia conflict.

Figure 10 shows a comparative analysis of the annual LNG and NH_3 fuel costs, including the carbon tax. In particular, the annual LNG fuel cost rises due to the reflection of the carbon tax. When the carbon tax is USD 50/ton, the LNG fuel is always more economical than the NH_3 fuel. If the carbon tax rises to USD 200/ton, the annual LNG fuel cost is estimated to be USD 40.8 million. Given that the annual fuel cost is USD 53.5 million in the case that the price of NH_3 is USD 500/ton, the economic feasibility of the NH_3 fuel is considered meaningful when the NH_3 fuel price falls below USD 400/ton.

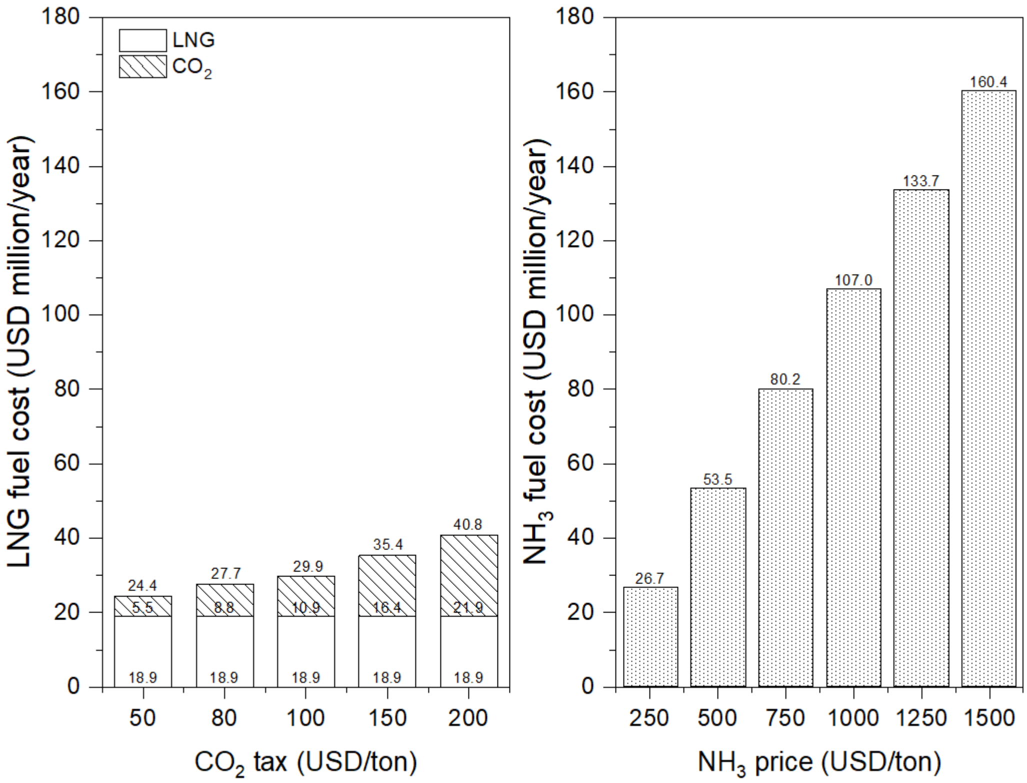

Figure 10. LNG and NH_3 fuel cost for the carbon tax and NH_3 price.

CAPEX is listed in Table 15. The price of a 15,000 TEU LNG-fueled container ship is approximately USD 142 million [37], and the supply cost of LNG fuel gas supply system (FGSS), including the fuel tank, is 10–25% of the ship's price [38]. The LNG FGSS cost of the fuel tank was calculated to be USD 21.3 million, and the NH_3 FSS cost was estimated at USD 10.65 million, half of the LNG FGSS cost.

Table 15. CAPEX of LNG FGSS and NH_3 FSS.

LNG FGSS, Million USD	NH_3 FSS Price, Million USD
21.3	10.65

In Figure 11, the results of the LCC for the carbon tax and the NH_3 price are illustrated. It can be seen that there is little effect of CAPEX in the LCC analysis. If the NH_3 price is more than USD 500/ton, it is not economical compared to LNG. When the NH_3 price is

USD 250/ton, and the carbon tax is over USD 80/ton, the NH_3 system is more economically feasible than the LNG one.

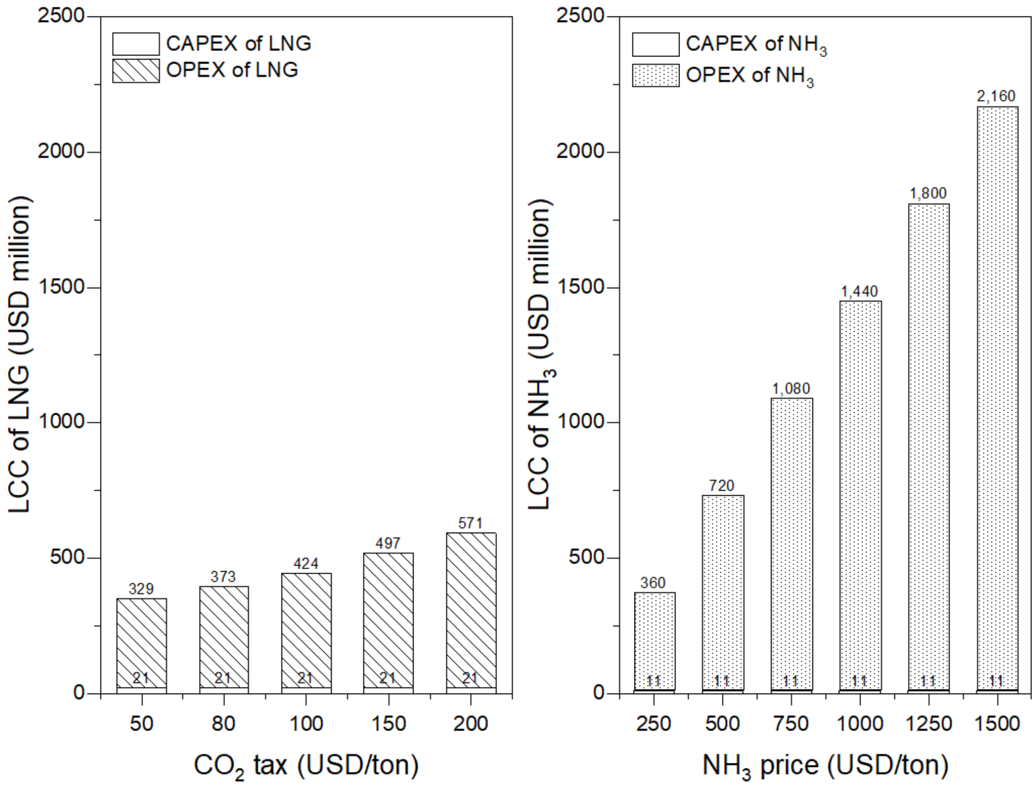

Figure 11. LCC of LNG and NH_3 for the carbon tax and NH_3 price.

4. Conclusions

This study proposed and economically evaluated the NH_3 fuel supply system and the re-liquefaction system for the 14,000 TEU ocean-going container ship. To handle the BOG, the re-liquefaction system was adopted with the vapor compression refrigeration cycle of the NH_3 refrigerant. The re-liquefaction system was assessed using thermodynamic performance analysis that estimated the energy and exergy efficiency and the economic feasibility that estimated the NPV. The exergy efficiency and SEC were 34.71% and 0.224 kWh/kg, respectively. In addition, the exergy destruction of each piece of equipment was reviewed. It was found that the exergy destruction of the heat exchangers and compressors accounted for 60% and 30% of the total exergy destruction, respectively. The NPV analysis revealed that if the NH_3 price drops to USD 250/ton, the USD 100 million-re-liquefaction system can make a profit in four years. Additionally, if the NH_3 price is USD 500/ton, the USD 200 million-re-liquefaction system can make a profit in four years. Considering that the cost of NH_3 falls to USD 250–300/ton, a re-liquefaction system cost between USD 0.5 and USD 1 million is reasonable.

The proposed FSS was designed to feed the liquid NH_3 at 80 bar and 40 °C and to re-feed the re-circulated NH_3 fuel with the sealing oil to the engine. The SEC of the FSS was investigated from 25% SMCR to 100% SMCR. The SEC ranged from 0.009 kWh/kg at 25% SMRC to 0.0063 kW at 100% SMCR.

Finally, the LCC and annual fuel costs for the NH_3 and LNG fuels were assessed. The carbon tax was included in the LNG fuel cost in this analysis. The annual LNG fuel cost for USD 50/ton, USD 80/ton, USD 100/ton, USD 150/ton, and USD 200/ton of the carbon tax was USD 24.4 million, USD 27.7 million, USD 29.9 million, USD 35.4 million, and USD 40.8 million, respectively. The average European carbon tax is USD 50/ton, and Switzerland and Sweden impose a carbon tax of USD 130/ton [39]. When the carbon tax is USD 50/ton, LNG fuel is always more economical than NH_3 fuel. If the carbon tax soars to USD 200/ton, the annual fuel cost of LNG will rise to USD 40.8 million. Given that the annual fuel cost is USD 53.5 million if the price of NH_3 is USD 500/ton, the economic feasibility of the NH_3 fuel is considered to be meaningful when the NH_3 fuel price falls below USD 400/ton. In addition, according to the results of the LCC analysis, the NH_3 fuel is economically feasible in the case that the carbon tax is more than USD 80/ton, and the NH_3 price is around USD 250/ton. According to reports, the future market price of NH_3 by 2050 is expected to be USD 250–400/ton [9,15,40–42]. This shows that the results of this study are significant.

Based on this study, NH_3 fuel is currently unattractive to economics. However, NH_3 is still estimated as a good candidate for future marine fuel. Therefore, the use of NH_3 as a marine fuel will increase as environmental regulations tighten. It is hoped that the results of this study will be an adequate reference for the research and development of NH_3-fueled ships and will significantly contribute to their commercialization. Although this study rationally derived design parameters as much as possible, it contains a certain level of uncertainties in economic and technical analyses. Many additional studies are needed to address these uncertainties. In addition, the development and early commercialization of NH_3 IC engines, NH_3 equipment, FSS, etc., will address these uncertainties. The authors will conduct further research by way of a rigorous LCC analysis and an optimal integrated system of an FSS and BOG management system based on the risk of NH_3.

Author Contributions: Conceptualization, J.L.; methodology, J.L.; software, J.L.; validation, J.L., Y.C. and J.C.; formal analysis, J.L.; investigation, J.L.; resources, J.L.; data curation, J.L.; writing—original draft preparation, J.L.; writing—review and editing, Y.C. and J.C.; visualization, J.L.; supervision, J.C.; project administration, J.C.; funding acquisition, J.C. All authors have read and agreed to the published version of the manuscript.

Funding: This work was supported by the Korea Institute of Energy Technology Evaluation and Planning (KETEP) grant funded by the Korean government (MOTIE) (Project No. 20223030030100, Development of web-based guidance platform technology for evaluation & design of fuel cell ships).

Institutional Review Board Statement: Not applicable.

Informed Consent Statement: Not applicable.

Data Availability Statement: Not applicable.

Conflicts of Interest: The authors declare no conflict of interest.

Nomenclature

$\dot{W}_{input}$	Work input
$\dot{W}_{net}$	Total work required to re-liquefy BOG
$\dot{W}_{Comp}$	Work input for the BOG compressor
$\dot{W}_{Ref\ 1}$	Work input for no. 1 refrigerant compressor
$\dot{W}_{Ref\ 2}$	Work input for no. 2 refrigerant compressor
$\dot{W}_{total}$	Total work required to supply the NH_3 fuel
$\dot{W}_{Submerged}$	Work input for the submerged pump
$\dot{W}_{HP}$	Work input for the HP pump
$\dot{W}_{GW}$	Work input for the GW pump
$\dot{m}$	Mass flowrate
$\dot{m}_{RLQ}$	Mass flowrate of re-liquified NH_3
$\dot{m}_{fuel}$	Mass flowrate of the NH_3 fuel
η_{ex}	Exergy efficiency
e	Specific exergy
$\dot{E}$	Physical flow exergy
$\dot{E}_{Cold-in}$	Physical cold flow-in exergy of heat exchanger
$\dot{E}_{Cold-out}$	Physical cold flow-out exergy of heat exchanger

$\dot{E}_{Hot-in}$	Physical hot flow-in exergy of heat exchanger
$\dot{E}_{Cold-out}$	Physical hot flow-out exergy of heat exchanger
$\dot{E}_{RLQ-in}$	Physical flow exergy of BOG of NH_3
$\dot{E}_{RLQ-out}$	Physical flow exergy of liquified NH_3
B_t	Benefit at t period in US dollars
C_t	Cost at t period in US dollars
C_D	Direct cost for CAPEX
C_{ID}	Indirect cost for CAPEX
C_{CF}	Contingency and fee for CAPEX
C_M	Cost of maintenance
C_F	Cost of fuel consumption
C_{CO2}	Cost of carbon dioxide
C_L	Cost of labor
L	Time span in years
M_{CO2}	Mass of carbon dioxide
R_{TAX}	Carbon tax
r	Discount rate in percent
t	Years

Abbreviations

ABS	American Bureau of Shipping
B/C	Benefit–cost
BOG	Boil-off Gas
BOR	Boil-off Rate
CAPEX	Capital Expenditure
CIF	Cost, Insurance, and Freight
CO_2	Carbon Dioxide
DF	Dual Fuel
DNV-GL	Det Norske Veritas and Germanischer Lloyd
EEDI	Energy Efficiency Design Index
EEOI	Energy Efficiency Operations Index
FGSS	Fuel Gas Supply System
FG	Fuel Gas Free on Board
FSS	Fuel Supply System
FVT	Fuel Valves Train
GHG	Green House Gas
GT	Gas Turbine
GW	Glycol Water
HFO	Heavy Fuel Oil
HP	High Pressure
IC	Internal Combustion
IEA	International Energy Agency
IMF	International Monetary Fund
IMO	International Marine Organization
IRR	Internal Rate of Return
ITF	International Transport Forum
KR	Korean Register
LCC	Lifecycle Cost
LH_2	Liquid Hydrogen
LHV	Lower Heating Value
LP	Low pressure
LUT	Lappeenranta University of Technology
(S)MCR	(Specific) Maximum Continuous Revolution
MEPC	Marine Environment Protection Committee
NCR	Nominal Continuous Revolution
NPV	Net Present Value

NPPD	Nebraska Public Power District
OPEX	Operating Expenditure
PEMFC	Proton-Exchange Membrane Fuel Cell
RVT	Return Valves Train
SEC	Specific Electric Consumption
SEEMP	Ship Energy Efficiency Management Plan
SFC	Specific Fuel Consumption
SFOC	Specific Fuel Oil Consumption
SHI	Samsung Heavy Industries
SOFC	Solid Oxide Fuel Cell

References

1. Sultanbekov, R.; Islamov, S.; Mardashov, D.; Beloglazov, I.; Hemmingsen, T. Research of the Influence of Marine Residual Fuel Composition on Sedimentation Due to Incompatibility. *J. Mar. Sci. Eng.* **2021**, *9*, 1067. [CrossRef]
2. Smyshlyaeva, K.I.; Rudko, V.A.; Povarov, V.G.; Shaidulina, A.A.; Efimov, I.; Gabdulkhakov, R.R.; Pyagay, I.N.; Speight, J.G. Influence of Asphaltenes on the Low-Sulphur Residual Marine Fuels' Stability. *J. Mar. Sci. Eng.* **2021**, *9*, 1235. [CrossRef]
3. Wu, P.C.; Lin, C.Y. Strategies for the Low Sulfur Policy of Imo—An Example of a Container Vessel Sailing through a European Route. *J. Mar. Sci. Eng.* **2021**, *9*, 1383. [CrossRef]
4. Cheliotis, M.; Boulougouris, E.; Trivyza, N.L.; Theotokatos, G.; Livanos, G.; Mantalos, G.; Stubos, A.; Stamatakis, E.; Venetsanos, A. Review on the Safe Use of Ammonia Fuel Cells in the Maritime Industry. *Energies* **2021**, *14*, 3023. [CrossRef]
5. Seo, Y.; Han, S. Economic Evaluation of an Ammonia-Fueled Ammonia Carrier Depending on Methods of Ammonia Fuel Storage. *Energies* **2021**, *14*, 8326. [CrossRef]
6. Bakhtov, A. *Alternative Fuels for Shipping in the Baltic Sea Region*; Helsinki Commission(HELCOM): Helsinki, Finland, 2019.
7. ITF/OECD. *Decarbonising Maritime Transport. Pathways to Zero-Carbon Shipping by 2035*; OECD: Paris, France, 2018.
8. Lewis, J. *Fuels Without Carbon-Prospects and the Pathway Forward for Zero-Carbon Hydrogen and Ammonia Fuel*; Clean Air Task Force: Boston, MA, USA, 2018.
9. IEA. *The Future of Hydrogen-Seizing Today's Opportunities*; International Energy Agency(IEA): Paris, France, 2019.
10. van Biert, L.; Godjevac, M.; Visser, K.; Aravind, P.V. A Review of Fuel Cell Systems for Maritime Applications. *J. Power Sources* **2016**, *327*, 345–364. [CrossRef]
11. Kim, K.; Roh, G.; Kim, W.; Chun, K. A Preliminary Study on an Alternative Ship Propulsion System Fueled by Ammonia: Environmental and Economic Assessments. *J. Mar. Sci. Eng.* **2020**, *8*, 183. [CrossRef]
12. Zincir, B. A Short Review of Ammonia as an Alternative Marine Fuel for Decarbonised Maritime Transportation. In Proceedings of the International Conference on Energy, Environment and Storage of Energy (ICEESEN2020), Kayseri, Turkey, 19–21 November 2020; pp. 19–21.
13. The American Bureau of Shipping(ABS). *Ammonia As Marine Fuel*; ABS: Houston, TX, USA, 2020.
14. Brinks, H.; Hektor, E.A. *Ammonia as a Marine Fuel*; DNV-GL: Hovik, Nrway, 2020.
15. Korean Register(KR). *Report on Ammonia-Fueled Ships*; KR: Busan, Korea, 2021.
16. Korean Register(KR). *Guidelines for Ships Using Ammonia as Fuels*; KR: Busan, Korea, 2021.
17. MAN ES. *MAN B&W Two-Stroke Engine Operating on Ammonia*; MAN ES: Copenhagen SV, Denmark, 2019.
18. MAN ES. MAN ES Targets 2024 for Delivery of First Ammonia Engine. Available online: https://www.motorship.com/man-es-targets-2024-for-delivery-of-first-ammonia-engine/1258700.article (accessed on 3 September 2022).
19. MAN ES. *Propulsion of 14,000 Teu Container Vessels*; MAN ES: Copenhagen SV, Denmark, 2020.
20. WARTSILA KOREA. Wärtsilä and SHI Agree to Collaborate on Ammonia Fuelled Engines for Future Newbuilds. Available online: https://www.wartsila.com/kor/media/news/22-09-2021-wärtsilä-and-shi-agree-to-collaborate-on-ammonia-fuelled-engines-for-future-newbuilds (accessed on 3 September 2022).
21. Trivyza, N.L.; Cheliotis, M.; Boulougouris, E.; Theotokatos, G. Safety and Reliability Analysis of an Ammonia-Powered Fuel-Cell System. *Safety* **2021**, *7*, 80. [CrossRef]
22. Aabo, K. Ammonia-Fuelled MAN B&W 2-Stroke Dual-Fuel Engines. *Mar. Eng.* **2020**, *55*, 737–744. [CrossRef]
23. Duong, P.A.; Ryu, B.; Jung, J.; Kang, H. Thermal Evaluation of a Novel Integrated System Based on Solid Oxide Fuel Cells and Combined Heat and Power Production Using Ammonia as Fuel. *Appl. Sci.* **2022**, *12*, 6287. [CrossRef]
24. SPLASH. Existing GTT LNG Containment System Can Be Used to Store Ammonia. Available online: https://splash247.com/existing-gtt-lng-containment-system-can-be-used-to-store-ammonia/ (accessed on 5 May 2022).
25. SAFETY4SEA. 2021 Was a Record Year for LNG Fueled Ships, Says DNV. Available online: https://safety4sea.com/2021-was-a-record-year-for-lng-fueled-ships-says-dnv/ (accessed on 4 September 2022).
26. Kim, T.W.; Suh, Y.S.; Jang, K.B.; Chun, M.S.; Lee, K.D.; Cha, K.H. A Study and Design on Tank Container for Fuel Tank of LNG Fueled Ship. *J. Soc. Nav. Archit. Korea* **2012**, *49*, 504–511. [CrossRef]
27. MAN ES. *CEAS Engine Data Report*; MAN ES: Copenhagen SV, Denmark, 2022.
28. Riviera. World's First LNG-Fuelled ULCS Joins CMA CGM Fleet. Available online: https://www.rivieramm.com/news-content-hub/news-content-hub/worldrsquos-first-lng-fuelled-vlcs-joins-cma-cgm-fleet-60937 (accessed on 4 September 2022).

29. Prem Baboo Ammonia Storage Tank Pre-Commissioning. *Int. J. Eng. Res.* **2019**, *8*, 612–624. [CrossRef]
30. Blanchard, J. *Storage of Liquefied Anhydrous Ammonia*; CB&I: Houston, TX, USA, 2007.
31. MAN ES. *MAN B&W ME-LGIP Dual-Fuel Engines*; MAN ES: Copenhagen SV, Denmark, 2018.
32. Lee, H.; Shao, Y.; Lee, S.; Roh, G.; Chun, K.; Kang, H. Analysis and Assessment of Partial Re-Liquefaction System for Liquefied Hydrogen Tankers Using Liquefied Natural Gas (LNG)and H2 Hybrid Propulsion. *Int. J. Hydrog. Energy* **2019**, *44*, 15056–15071. [CrossRef]
33. Adachi, M.; Kosaka, H.; Fukuda, T.; Ohashi, S.; Harumi, K. Economic Analysis of Trans-Ocean LNG-Fueled Container Ship. *J. Mar. Sci. Technol.* **2014**, *19*, 470–478. [CrossRef]
34. Turton, R.; Bailie, R.C.; Whiting, W.B.; Shaeiwitz, J.A. *Analysis, Systhesis, and Design of Chemical Processes*, 4th ed.; Prentice Hall: Upper Saddle River, NJ, USA, 2012.
35. IMO MEPC. *RESOLUTION MEPC.281(70) (Adopted on 28 October 2016) AMENDMENTS*; IMO: London, UK, 2016.
36. Thoft-Christensen, P. Infrastructures and Life-Cycle Cost-Benefit Analysis. *Struct. Infrastruct. Eng.* **2012**, *8*, 507–513. [CrossRef]
37. PULSE. Samsung Heavy Industries Grabs $710 Mn LNG-Fueled Container Ship Order. Available online: https://pulsenews.co.kr/view.php?sc=30800021&year=2021&no=151388 (accessed on 4 September 2022).
38. Yoo, B.Y. Economic Assessment of Liquefied Natural Gas (LNG) as a Marine Fuel for CO_2 Carriers Compared to Marine Gas Oil (MGO). *Energy* **2017**, *121*, 772–780. [CrossRef]
39. Bray, S. Carbon Taxes in Europe. Available online: https://taxfoundation.org/carbon-taxes-in-europe-2022/ (accessed on 3 September 2022).
40. Laval, A.; Hanfia; Topsøe, H.; Vestas; Gamesa, S. *Ammonfuel—An Industrial View of Ammonia as a Marine Fuel*; Alfa Laval: Lund, Sweden, 2020.
41. Blanco, H.; Jinks, B.; Bianco, E.; Sezer, U. Innovation Outlook Renewable Ammonia in Partnership with about Irena Valuable Review and Feedback Was also Provided by Irena Colleagues Renewable Ammonia 3 Contents. 2022. Available online: https://www.irena.org/publications/2022/May/Innovation-Outlook-Renewable-Ammonia (accessed on 4 September 2022); ISBN 978-92-9260-423-3.
42. Bunro Schiozawa. The Cost of CO_2-Free Ammonia. Available online: https://www.ammoniaenergy.org/articles/the-cost-of-co2-free-ammonia/ (accessed on 4 September 2022).